

## FURTHER INSIGHTS OF TEMPERATURE-TIME EVENTS ON HED PARENT BODY USING U-TH-PB CHRONOLOGY OF ZIRCON-BEARING NORITIC DIOGENITE NORTHWEST AFRICA 10666.

C. Martinez<sup>1</sup>, M. Righter<sup>1</sup>, T. J. Lapen, and A. J. Irving<sup>2</sup>, <sup>1</sup>Dept. of Earth and Atmospheric Sciences, University of Houston, TX, USA (mrighter@uh.edu), <sup>2</sup>Dept. of Earth & Space Sciences, University of Washington, Seattle, WA, USA.

**Introduction:** The Howardite-Eucrite-Diogenite (HED) meteorites are a clan of achondrites believed to be derived from asteroid 4 Vesta located in the asteroid belt between Mars and Jupiter [1]. The HED parent body underwent accretion and differentiation very early in solar system history (4563-4565 Ma) [e.g. 2-4], experienced igneous activity for perhaps its first 50 Ma [e.g. 5], and was subjected to significant impacts, perhaps culminating between 4.1 and 3.3 Ga [e.g. 6-7].

Diogenites are coarse-grained, ultramafic igneous rocks characterized as orthopyroxene-rich with smaller, but variable abundances of clinopyroxene, plagioclase, chromite, and olivine [8-9]. Many diogenite specimens are cataclastic, although some samples such as Dhofar 700 are classified as unbrecciated. These meteorites are important because they serve as records of lower crustal processes in the parent body [10]. Constraints on the temperature-time histories of lower-crustal materials have been difficult to constrain due to limited chronologic options for these typically mineralogical simple meteorites in addition to thermal equilibration/metamorphism.

NWA 10666 is one among a series of noritic and feldspathic diogenites and the first reported zircon-bearing diogenite [8-9,11]. The meteorite also contains Cl-apatite, making this specimen well suited for multi-chronometric approaches to understand high and low temperature thermal history. Here, we present *in situ* U-Th-Pb chronology of zircon and Cl-apatite to better constrain its temperature-time history of diogenite NWA 10666.

**Sample and Analytical Techniques:** A ~2mm thick polished section was prepared for this study. *In situ* dating of zircon and apatite was conducted by a Photon Machines *Excite* laser ablation system coupled to a Varian 810 quadrupole ICP-MS at University of Houston. The laser ablation will be completed using 25  $\mu\text{m}$  spot sizes with repetition rate of 8-10 Hz and an energy output of 3 J/cm<sup>2</sup>. Individual spot analyses are 60 seconds in length and are split into three parts with each lasting approximately 20 seconds: background measurements, ablation and wash-out. For zircon chronology, the Plešovice and zircon megacryst from Rio de Peixe, Brasil were used as the external calibration standard and the FC5z zircon as the internal standard. With this system we can consistently measure U-Pb ages of zircons within 1.5% of their known TIMS

age and can routinely achieve precisions of pooled ages of  $\pm \sim 0.3\%$  ( $2\sigma$ ) and 1-7% for individual spot analyses, depending on U concentration, age, and grain size. For apatite chronology, the Bear Lake apatite was used as the external calibration standard and Yates Mine as the internal standard for instrumental U-Pb and Th-Pb elemental fractionation corrections. Instrumental mass fractionation of Pb isotopes were corrected with NIST 612 glass.

**Results:** Three U-Th-Pb analyses were conducted on a fragmented large (~100 $\mu\text{m}$ ) zircon grain within the thick section of NWA 10666. This zircon is adjacent to anhedral ilmenite grains and has ilmenite inclusions. The U and Th concentrations of zircon are very low, ranging from 9-11 ppm and 0.3-0.4 ppm, respectively. The three analyses yielded <sup>207</sup>Pb-<sup>206</sup>Pb ages of 4532  $\pm$  34 Ma, 4566  $\pm$  36 Ma, and 4570  $\pm$  40 Ma producing a <sup>207</sup>Pb-<sup>206</sup>Pb weighted average age of 4555  $\pm$  21 Ma (MSWD = 1.4) (Fig 2). Because the analyzed zircon is heavily fractured, common Pb contamination along cracks is possible. A <sup>204</sup>Pb/<sup>206</sup>Pb – <sup>207</sup>Pb/<sup>206</sup>Pb inverse isochron yields an age of 4542  $\pm$  20 Ma (MSWD = 0.29) (Fig. 3), slightly younger than, but statistically identical to the weighted average <sup>207</sup>Pb/<sup>206</sup>Pb age, indicating that common Pb contamination is not an issue that is resolvable in the data. A U-Pb concordia upper intercept age of 4576  $\pm$  29 (MSWD = 0.09) is determined; 2 out of 3 data points are reversely discordant. Based on the fractured nature of the zircon and potential for Pb contamination, the inverse isochron age of 4542  $\pm$  20 is interpreted to be the most accurate age of zircon crystallization.

A total of four analyses were made on four separate Ca-phosphate grains, each being larger than 35 $\mu\text{m}$  in their smallest dimension. Two of them were surrounded by plagioclase and the other two grains were surrounded by pyroxene. The phosphates contain uranium and thorium concentrations of 22- 33 ppm and 1499- 2568 ppm, respectively. The <sup>207</sup>Pb- <sup>206</sup>Pb ages of the four spots are 4267  $\pm$  41, 4240  $\pm$  65, 4238  $\pm$  33, and 4313  $\pm$  38 Ma and these data yield a weighted mean age of 4271  $\pm$  28 Ma (MSWD = 2.6). Given the potential for common Pb inherent within phosphate, the Pb data is presented as a <sup>204</sup>Pb/<sup>206</sup>Pb – <sup>207</sup>Pb/<sup>206</sup>Pb inverse isochron (Fig. 4) which yields an intercept age of 4248  $\pm$  25 Ma (MSWD = 1.5). This is slightly younger but within

uncertainty than the  $^{207}\text{Pb}$ - $^{206}\text{Pb}$  weighted mean age, indicating that the effects of common Pb are not a significant issue. The U-Pb data yield a concordia intercept age of  $4271 \pm 28$  Ma (MSWD = 2.6), also identical within uncertainty with the weighted average  $^{207}\text{Pb}$ - $^{206}\text{Pb}$  and inverse isochron ages. Despite the overlapping ages, the age determined by the inverse isochron method is regarded as the most accurate given that it addresses any issues with common Pb.  $^{232}\text{Th}$ - $^{208}\text{Pb}$  ages are  $4103 \pm 120$ ,  $4350 \pm 254$ ,  $4203 \pm 108$ , and  $4259 \pm 111$  Ma with a weighted average of  $4202 \pm 63$  Ma, also identical to the Pb-Pb and U-Pb ages.

**Discussion:** Since zircons have not been recorded in any other diogenites, comparison has been made with cumulate and basaltic eucrites. The  $4542 \pm 20$  Ma zircon age of NWA 10666 is coeval with eucrite U-Pb in zircon ages within uncertainty [12-14]. These ages indicate that eucrite-diogenite crystallized from parental magmas within a short interval following the differentiation of the parent body. The apatite U-Pb chronology indicates a significant heating event at 4200 Ma, a date that falls outside most measurements with low-temperature chronometers such as Ar-Ar. It is unlikely that the parent body remained above the closure temperature of Pb in apatite for 300 m.y. after formation; the apatite age most likely reflects a thermal metamorphic event associated with impacts. U-Pb in zircon was not affected by the Pb-loss/recrystallization event recorded in the phosphate. Presumably, lower energy metamorphic events <4.0 Ga reset the Ar-Ar dates in silicates, but not the U-Pb in phosphates. The 3.3-3.8 Ga may reflect an overall waning impact intensity in the inner Solar System. Thus, U-Pb in phosphates may be a window into determining the timing of metamorphic events between igneous crystallization and Ar-Ar dates that indicate impact cataclysm.

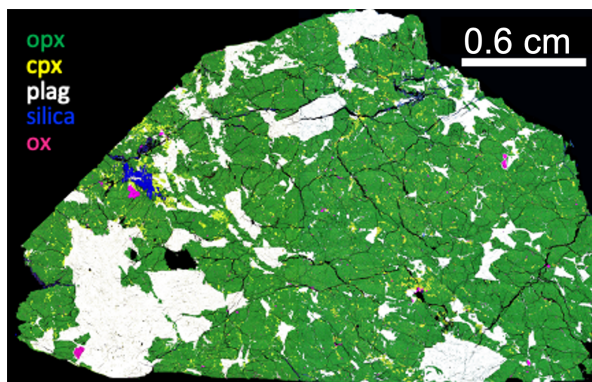


Fig. 1. Chemical map of NWA 10666. Orthopyroxene (“opx”, dark green); Clinopyroxene (“cpx”, yellow-green); Plagioclase (“plag”, white); oxides (“ox”, magenta); and Silica (“silica”, blue).

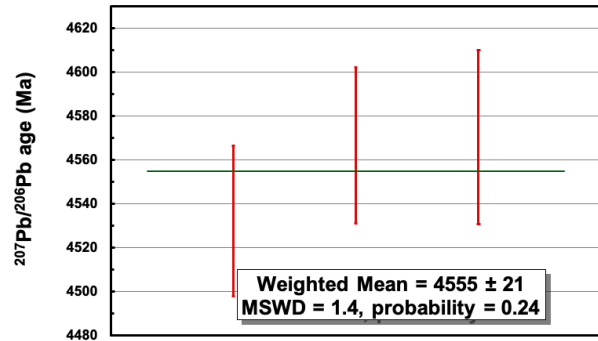


Fig. 2. The  $^{207}\text{Pb}$ - $^{206}\text{Pb}$  ages for three zircon grains. The weighted mean age is  $4555 \pm 21$  Ma.

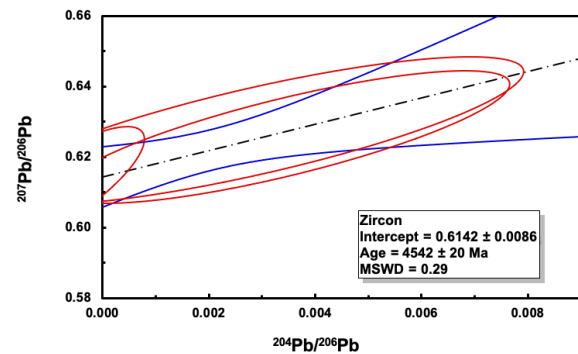


Fig. 3. Plot of  $^{207}\text{Pb}/^{206}\text{Pb}$  versus  $^{204}\text{Pb}/^{206}\text{Pb}$  ratios for three zircon spots.

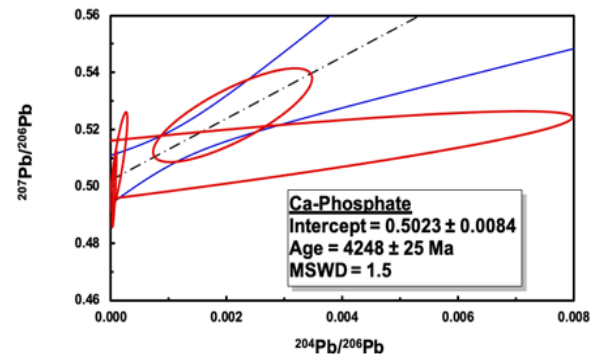


Fig. 4. Pb-Pb inverse isochron diagram for Ca-phosphates.

**References:** [1] McSween H.Y. et al. (2013) *Meteorit. & Plant. Sci.*, 48, 2019–2104. [2] Kleine T. et al. (2009) *GCA* 73, 5150–5188. [3] Trinquier et al. (2008) *GCA* 72, 5146–5163. [4] Schiller M. et al. (2011) *GCA* 74, 4844–4864. [5] Zhou Q. et al. (2013) *GCA* 110, 152–175. [6] Bogard D.D. and Garrison D.H. (2003) *Meteorit. & Plant. Sci.*, 38, 669–710. [7] Cohen B.A. (2013) *Meteorit. & Plant. Sci.*, 1–15. [8] Irving A.J. et al. (2014) *77th Meteorit. Soc. Mtg.*, #5199. [9] Irving A.J. et al. (2016) *LPS XLVII*, #2264. [10] Mittlefehldt D.W. et al. (2012) *Meteorit. & Plant. Sci.*, 47, 72–98. [11] Tanner T.B. et al. (2017) *LPS XLVIII*, #2714. [12] Misawa K. et al. (2005) *GCA* 69, 5847–5861. [13] Zhou Q. et al. (2013) *GCA* 110, 152–175. [14] Izuka T. et al. (2015) *EPSL* 409, 182–192.